Technical University of Denmark

Link-Placement Characterization of Optical Phase Conjugation for Nonlinearity Compensation

Da Ros, Francesco; Yankov, Metodi Plamenov; Porto da Silva, Edson; Lillieholm, Mads; Forchhammer, Søren; Galili, Michael; Oxenløwe, Leif Katsuo

DTU Library
Technical Information Center of Denmark

Link-Placement Characterization of Optical Phase Conjugation for Nonlinearity Compensation

F. Da Ros, M.P. Yankov, E.P. da Silva, M. Lillieholm, S. Forchhammer, M. Galili, L.K. Oxenløwe

DTU Fotonik, Technical University of Denmark, DK-2800 Kongens Lyngby, Denmark, fdro@fotonik.dtu.dk

Abstract: The impact of the OPC offset on the nonlinearity compensation is experimentally investigated, achieving gains up to 0.6-dB SNR and 0.17-bit/symbol mutual information with optimal mid-link OPC for dispersion-compensated transmission up to 966 km. © 2018 The Author(s)
OCIS codes: (060.4510) Optical communications; (190.4380) Nonlinear optics, four-wave mixing,

1. Introduction

The impact of Kerr nonlinearity currently limits the performance of coherent transmission systems. A strong research effort has therefore been directed towards techniques for mitigation or at compensation of the nonlinear distortion experienced by signals during transmission. While techniques based on digital signal processing (DSP) are particularly effective in compensating for intra-channel nonlinearity, analog bandwidth limitations make them impractical for addressing inter-channel nonlinear distortion [1]. All-optical techniques, instead, may be more suited for tackling cross-channel nonlinearity due to their larger operation bandwidth. Amongst them, in-line optical phase conjugation (OPC) has been proven effective for nonlinearity compensation. Several impressive demonstrations show significant improvement achieving bandwidths up to 2.3 THz [2].

The improvement provided by in-line OPC for compensation of Kerr nonlinearity is however strongly dependent on the transmission link fulfilling rather stringent dispersion and power symmetry requirements [3]. These requirements limit the practical link configurations where compensation is achieved. Dispersion-managed transmission with lumped erbium-doped fiber amplifiers (EDFAs) or links with distributed Raman amplification can provide sufficient symmetry to enable performance improvement by mid-link OPC [3-5].

In a practical scenario, implementing the OPC operation at the exact mid-point in a link may not be possible or desirable. Hence, the impact of OPC position on the nonlinearity compensation has been numerically investigated for dispersion-unmanaged links in [1, 6, 7]. Additionally, in [1, 7], the potential to compensate for an offset in OPC position by lower complexity DBP has been proposed and numerically evaluated.

In this work, we provide an experimental analysis of the impact of the OPC position on the achievable improvement in mutual information (MI) and the effective receiver signal-to-noise ratio (SNR) for dispersion-compensated transmission up to 966 km. The position of the OPC is varied in steps of 161 km and the performance for 16-GBd 64- quadrature amplitude modulation (QAM) is benchmarked against straight (without OPC) transmission in a 5-channel wavelength division multiplexing (WDM) scenario.
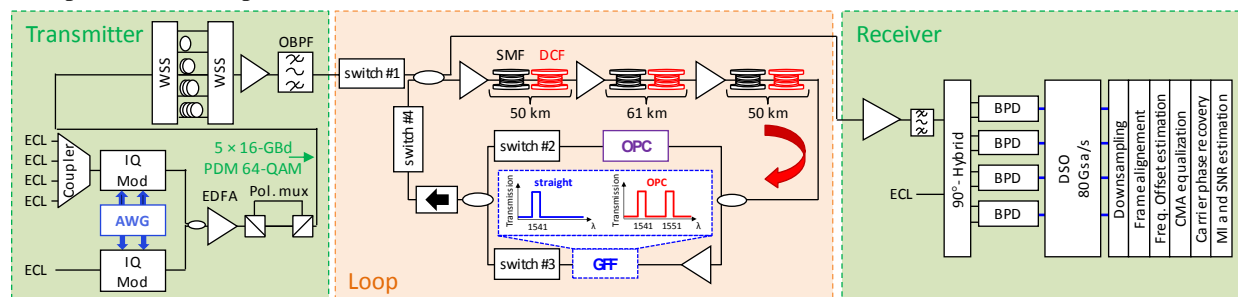
2. Experimental setup

Fig. 1. (a) Experimental setup for the dispersion-compensated transmission with OPC: inset shows the transmission profiles for the GFF opening only the signal band and both signal and idler band for straight and OPC-based transmissions, respectively.

The experimental setup is shown in Fig. 1. Five external cavity lasers (ECLs) are modulated in two IQ modulators (one for the central channel under test, one for the four interferers) driven by an arbitrary waveform generator (AWG, 64 GSa/s) operating at 16 GBd. The waveform loaded in the AWG consists of random data mapped into a 64-QAM constellation and interleaved with quadrature phase shift keying (QPSK) pilot symbols, used for equalization and phase noise tracking, at a pilot rate of 10%. A root-raised cosine pulse shaping (roll-off of 0.01) is applied. After modulation, a polarization division multiplexed (PDM) signal is generated with a delay-and-add polarization multiplexing emulator. The five channels are individually decorrelated using wavelength selective

switches (WSSs) and fiber delays (delay>50 symbols), and then injected into the transmission link. The link is based on a recirculating loop setup consisting of three dispersion-compensated spans (loop length of 161 km), combining single mode fiber (SMF) and dispersion compensating fiber (DCF). Span losses are compensated by EDFAs which are used to vary the launch power at the input of each span. For every loop turn, two acousto-optic switches control if the signal is conjugated in the OPC setup (*switch #2 closed*) or simply amplified in an EDFA followed by a programmable gain-flattening filter (GFF) which suppresses out-of-band amplified spontaneous emission (ASE) noise (*switch #3 closed*). As shown in the inset of Fig. 1, for straight transmission the GFF selects and flattens a 4-nm bandwidth around the signal wavelength (1540.75 nm). For the OPC-based transmission, the GFF selects two 4-nm bands, one for the signal and one for the idler. This requires a more careful balance of the attenuation of the two bands and results in a noise band always co-propagating with the signal/idler band (the impact of this effect on the overall transmission performance is discussed below). After transmission, the central channel is received with a pre-amplified coherent receiver based on a digital sampling oscilloscope (DSO, 80 GSa/s) and off-line DSP consisting of (in order) frequency offset estimation, pilot-aided equalization [8], phase recovery and MI and SNR estimation [9]. The MI is estimated by using an auxiliary probability distribution derived by the phase recovery algorithm [9]. The estimations are carried out over 10^6 symbols leading to a measurement precision better than 0.05 bit/symbol and 0.1 dB for MI and SNR, respectively.
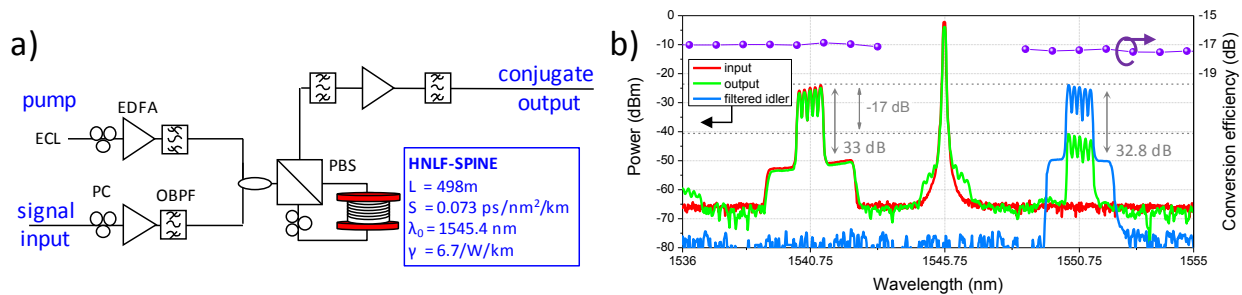

Fig. 2. (a) Setup of polarization-diversity based OPC module and (b) OPC input and output spectra, and CE of the HNLF-SPINE.

The OPC configuration is shown in Fig. 2(a). The WDM channels and a continuous wave (CW) pump from an ECL are separately amplified and band pass filtered before coupling them together at the input of a polarization-diversity loop based on a polarization beam splitter (PBS) and a highly nonlinear fiber (HNLF). Four-wave mixing (FWM) in the HNLF performs the OPC operation. The pump wavelength and power at the HNLF input have been optimized to 1545.75 nm and 22 dBm (per propagation direction), respectively, leading to a flat conversion efficiency (CE) of -17 dB over most of the C-band. Fig. 2(b) shows the CE measured by sweeping the wavelength of a single CW signal at the input of the OPC. Polarization dependence below 0.4 dB is achieved. The total input signal power has been optimized to 2 dBm, as a trade-off between optical signal-to-noise ratio (OSNR) degradation and nonlinear distortion [10]. The input and output spectra for the 5×WDM channels after 322-km transmission are shown in Fig. 2(b). The observed spectral tilt of both signal and idler bands is due to sub-optimum gain flattening. Negligible OSNR penalty (< 0.2 dB) is introduced by the conversion as seen comparing input signal to output idler after amplification and optical bandpass filtering (OBPF). Finally, the use of a high-quality (10-kHz linewidth) pump laser further ensures a negligible penalty due to pump phase noise transfer [10].

3. Transmission results

The MI has been measured as a function of the total launched power at the input of each span and the results are shown in Fig. 3(a) and 3(b) for 644-km (4 loop turns) and 966-km (6 loop turns) transmission, respectively. The position of the OPC has been varied in steps of one loop turn (161 km) and the measured MI is benchmarked against straight transmission. In the *nonlinear transmission regime* (P_{launch}> -3 dBm), the MI with OPC is always higher than for straight transmission (black dashed curves) regardless of the OPC position. However, the MI improvement is inversely proportional to the OPC offset from mid-link operation (red curves). At the *optimum launched power*, mid-link OPC provides an MI improvement of up to 0.17 bit/symbol and an SNR gain of 0.6 dB. Such an improvement decreases when the position of the OPC is shifted away from the mid-point. Additionally, the optimum launched power for the mid-link OPC is increased by 2 dB compared to straight transmission. In the *linear transmission regime* (P_{launch}< -6 dBm), the measured MI is unaffected by the presence of the OPC (compared to straight transmission), as long as the OPC is not positioned beyond the link mid-point. This further highlights that the conjugation does not induce significant penalty to the signal. When the OPC operation is shifted towards the end of the link, i.e. beyond the mid-point, the performance in the linear regime is degraded due to signal OSNR degradation prior to the conjugation stage. Due to the GFF configuration in our setup (Fig. 1), an ASE noise band

co-propagates with the signals during the loop turns pre-OPC leading to additional OSNR degradation through gain competition in the in-line EDFA. As this effect is artificial and specific to our recirculating setup and would not impact an in-line transmission system, the measurements provide a lower bound on the achievable improvement for OPC positions beyond the link mid-point. For straight transmission, only the signal band is selected in the GFF.

The overall improvements in both received MI and SNR are summarized in Fig. 3(c) and (d), respectively. As expected for this link configuration [3], the maximum improvement is achieved for mid-link OPC operation, however, offsetting the OPC by ±0.17·L (one span for 966-km transmission) still provides MI and SNR improvements. These results are in agreement with the numerical predictions of [6]. Additionally, a sub-optimum position of the OPC could be mitigated by combining OPC and low-complexity DBP as discussed in [7, 11].
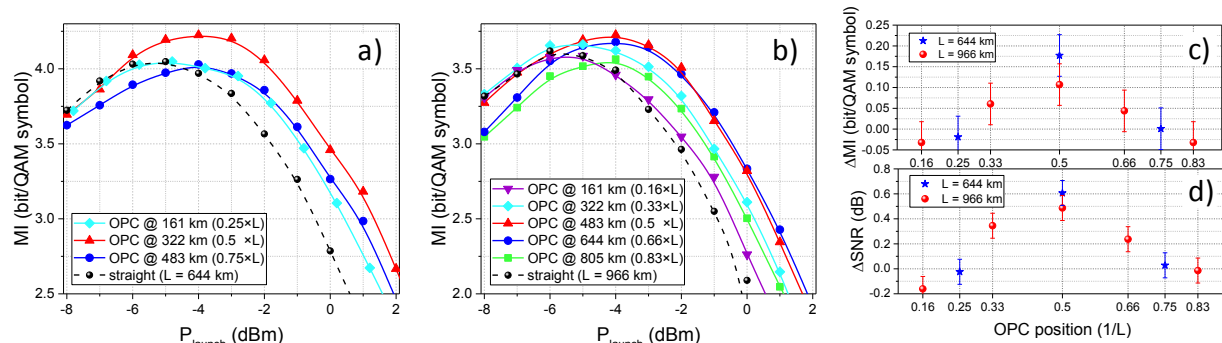

Fig. 3. MI as a function of the launched power for straight and OPC-based transmission for different OPC positions and a total transmission distance of 644 km (a) and 966 km (b). Improvements in MI (c) and SNR (d) as functions of the OPC position for both transmission distances. All measurements refer to the central channel.

4. Conclusions

We have investigated the improvement provided by OPC for dispersion-compensated transmission of a 5×WDM PDM 64-QAM signal for up to 966 km transmission. The impact of the OPC position on the nonlinearity compensation performance has been evaluated in terms of receiver MI and effective SNR demonstrating a gain in performance provided by the nonlinearity compensation, which decreases with the offset of the OPC from the link mid-point. Nevertheless, the increased nonlinearity tolerance in the nonlinear transmission regime is clearly visible for all of the evaluated OPC positions.

5. Acknowledgements

6. References

[1] J. Cartledge, *et al.,* "Signal processing techniques for reducing the impact of fiber nonlinearities on system performance," in Proc. OFC 2016, paper Th4F.5.

[2] T. Umeki, *et al.,* "Simultaneous nonlinearity mitigation in 92 × 180-Gbit/s PDM-16QAM transmission over 3840 km using PPLN-based guard-band-less optical phase conjugation," Optics Express **24**(15), 16945-16951 (2016).

[3] P. Minzoni, "Nonlinearity compensation in a fiber-optic link by optical phase conjugation," Fiber and Integrated Optics **28**(3), 179-209 (2009).

[4] A.D. Ellis, *et al.,* "4 Tb/s transmission reach enhancement using 10 × 400 Gb/s super-channels and polarization insensitive dual band optical phase conjugation," Journal of Lightwave Technology **34**(8), 1717-1723 (2016).

[5] Y. Sun, *et al.,* "Optical nonlinearity mitigation of 6×10GBd polarization-division multiplexing 16-QAM signals in a field-installed transmission link," in Proc. OFC 2017, paper Th3J.2.

[6] K. Solis-Trapala, *et al.*, "Doubled transmission reach for DP-64QAM signal over field-deployed legacy fiber systems enabled by MSSI," in Proc. ECOC 2015, paper Mo.3.6.2.

[7] I. Kim, *et al.,* "Impact of link symmetry on nonlinear noise mitigation using spectral inversion in superchannel transmission," in Proc. OECC/PS 2016, paper TuB3-2.

[8] D. Rafique, and A.D. Ellis, "Various nonlinearity mitigation techniques employing optical and electronic approaches," Photonics Technology Letters **23**(23), 1838-1840 (2011).

[9] M.P. Yankov, *et al.*, "Experimental analysis of pilot-based equalization for probabilistically shaped WDM systems with 256QAM/1024QAM," in Proc. OFC 2017, paper W.2.A.48.

[10] M.P. Yankov, *et al.,* "Constellation shaping for WDM systems using 256QAM/1024QAM with probabilistic optimization," Journal of Lightwave Technology **32**(22), 5146-5156 (2016).

[11] F. Da Ros, *et al.,* "Impact of signal-conjugate wavelength shift on optical phase conjugation-based transmission of QAM signals," in Proc. ECOC 2017, paper P1.SC4.66.